Podosomes display actin turnover and dynamic self-organization in osteoclasts expressing actin-GFP.

Olivier Destaing, Frédéric Saltel, Jean-Christophe Géminard, Pierre Jurdic and Frédéric Bard

Supplementary Material.

Theoretical model of the podosome.

Introduction: polymerization at the base and severing at the heart.

In live confocal microscopy, podosomes present a steady shape during their two to three minutes life-span as indicated by a constant actin-GFP fluorescence signal. FRAP experiments indicate however that actin-GFP is constantly added and removed at a rate sufficient to replace about half of the structure in 30 seconds. This proves therefore that the podosome is a dynamical structure and raises the question of the mechanisms involved. Polymerization is by far the most likely event to explain the addition of actin in the structure and is consistent with the rapid disappearance of podosomes upon addition of the actin monomer sequestering drug latrunculin B (data not shown). By analogy with other structures where rapid actin turnover occurs, like the lamellipodia or actin comets (Pantaloni et al., 2001), we propose that polymerization occurs where Cortactin and WASP are localized, that is at the base of the podosome (Pfaff and Jurdic, 2001). Removal of actin could conceivably occur by two mechanisms: depolymerization at the top of the podosomes or severing of filaments at a certain rate randomly over their whole length. However, following photobleaching, the first mechanism would result in a linear recovery of the fluorescence (Fig. S1), and is therefore inconsistent with our experimental results. Moreover, such a process implies an external regulation mechanism in order to reach the stationary shape of the podosomes. By contrast, the second mechanism leads to an almost exponential recovery of the fluorescence, as described thereafter. Furthermore, the efficiency of this mechanism, being directly proportional to the length of the filaments (i.e. the number of bounds accessible to severing) provides a simple mean to reach a steady shape for the podosomes.

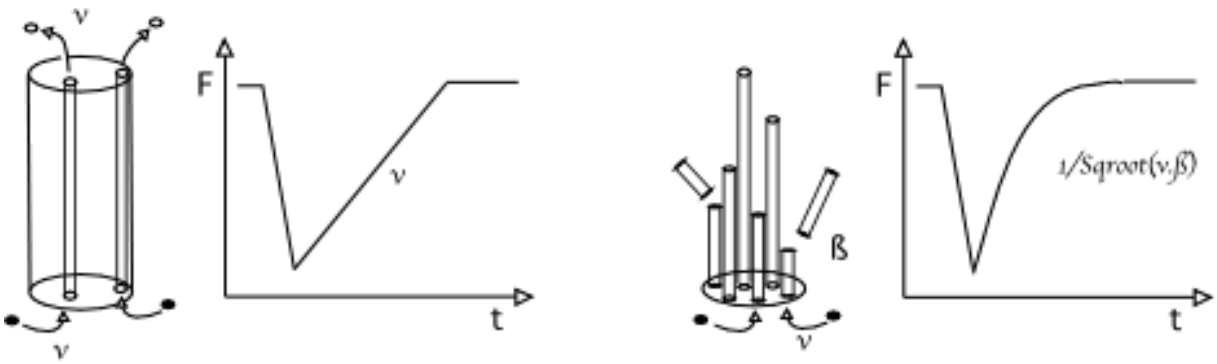

Fig. S1: Depolymerization and severing mechanisms result in different FRAP curves.
To ensure a regular turnover of the podosome, two mechanisms of actin removal can be hypothesized, but only severing would result in an exponential-shaped fluorescence recovery curve. The characteristic times depends on both polymerization speed and severing frequency as explained later.

Basic qualitative ingredients of the model

We first have to describe the synthesis of actin filaments that will occur in narrow regions of radius r_{podo} (about 0.15 μm). To account for the internal dynamics of the podosome, one has to consider, in the first place, that the length L of a single actin filament anchored to the basal cell membrane is increased, by addition of v monomers (size r_0) per unit time, according to $dL/dt = vr_0$. For the sake of simplicity, actin filaments are considered a linear bead tread, with an apparent diameter of monomers of 2.7 nm inside the filament (Pantaloni et al., 2001).
We then consider severing of the bounds between the monomers to occur at the frequency β. A filament constituted by n+1 monomers [length $L = (n+1)\, r_0$] is cut with the frequency nβ, that is proportional to the number of bounds n.

Let us now consider a whole podosome, constituted by M filaments. We assume that the packing of the filaments does not prevent both the monomers and the severing enzyme to access freely the filaments. Consistent with this assumption, we could detect by confocal imaging the enzyme gelsolin, for example, within the whole podosome structure (data not shown). We denote N(n;t) the number of filaments which length is $(n+1)\, r_0$ at time t, n being the number of bounds. The evolution in time of N(n;t), due to both the polymerization and the severing, then writes:

$$\frac{\partial N(n;t)}{\partial t} = v\,[\,N(n-1;t) - N(n;t)\,] - \beta\, n\, N(n;t) + \beta \sum_{i=n+1}^{\infty} N(i;t) \qquad (1)$$

The first term corresponds to the translation of the distribution of filaments due to the synthesis. The second and third terms come from the severing mechanism in two different ways. First, the filaments with n bounds are attacked at the frequency nβ. This leads to their

disappearance. Second, every filament with initially i bounds (i > n) is cut at the $(n+1)^{th}$ bound with the frequency β, leading to a new filament with n bounds.

Steady solution to the model: a brush of filaments of multiple sizes.

In the steady regime, the derivative with respect to time vanishes, and the steady distribution of the filaments writes (solution to Eq.1, with $\partial N(n;t)/\partial t = 0$):

$$N(n) = M \frac{\beta}{v} \frac{\Gamma(n+1)}{\prod_{i=0}^{n+1} \left(1 + \frac{\beta}{v} i \right)} \qquad (2)$$

The distribution N(n) only depends on the ratio v/β and reaches a maximum for $n = \sqrt{\frac{v}{\beta}}$. For M = 100, N(n) can be seen as the percentage of filaments containing n bounds (Fig.S2), and then having the length $L = (n+1)\, r_0$. There is then a steady characteristic length of the filaments that writes:

$$< L > = r_0 \left(1 + \sqrt{\frac{v}{b}} \right) \qquad (3)$$

These theoretical podosomes appear therefore as brushes of actin filaments whose lengths are distributed according to N(n). Synthesis and severing continuously occur and lead to large fluctuations of the length L of each filament, but, if we consider the whole podosome, the filaments have a characteristic length < L > that does not change in time and which does not depend on r_{podo}.

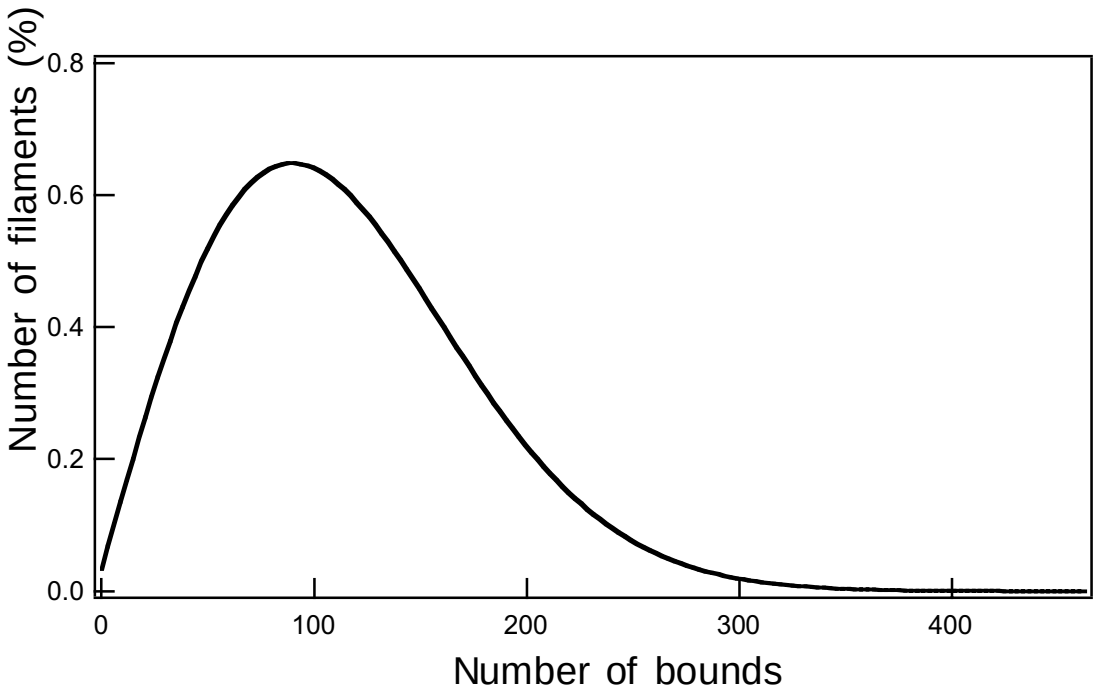

Figure S2: Percentage of filaments having the number of bounds n in the steady regime(M=100).

Random severing accounts for an apparent conical shaped podosome:

With the spatial resolution of the confocal microscope, the image of one podosome reduces to a bright spot. When imaging a layer perpendicular to the filaments and located at a height $h=nr_0$ from the cell membrane, the intensity of light I is proportional to the number of filaments that are long enough to intersect the plane, which can be written as $I(n) \propto \sum_{i=n}^{\infty} N(i)$

.We consider that the podosomes are compact structures because the actin filaments appear packed by electron microscopy (Nermut et al., 1991; Nitsch et al., 1989) and because bundling proteins like fimbrin were reported in the podosome (Babb et al., 1997). The light intensity I(n) can therefore be considered as proportional to the surface area of the horizontal section of the podosome at height h, that is to πr^2, r being the apparent radius of the podosome. From r proportionality to $\sqrt{I}$, we can deduce the apparent profile of the podosome given in Figure S3a. When the depth of focus of the confocal microscope is taken into account, the podosome presents a more conical shape. Furthermore, the upper part of the podosome is likely to be undetectable against the background of the cloud given that the light at h decreases like r^2. Overall, we think that our model could readily account for the conical aspect obtained by confocal microscopy optical z-section (see movie n° 1: 3D reconstruction of a cluster of podosomes).

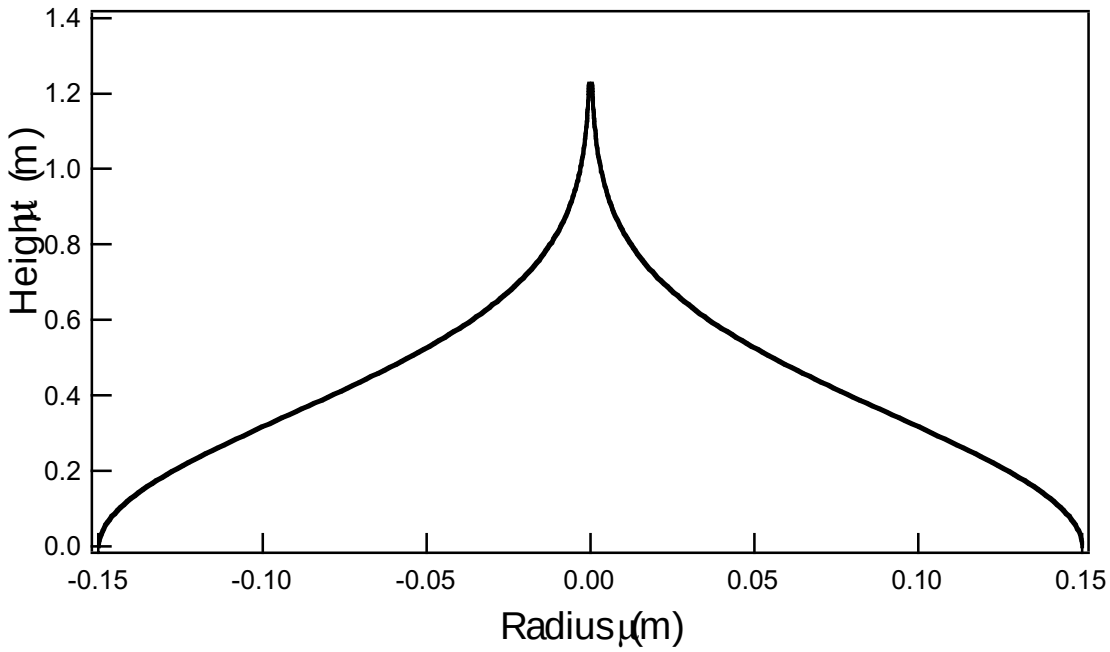

Figure S3: Theoretical apparent profile of a podosome.
This profile is obtained with a polymerisation frequency v = 3.1Hz Hz, the severing frequency β = 3.6 10^{-4} Hz, and r_{podo} = 0.15 μm.

Recovery after photobleaching: the model accounts for an exponential curve of FRAP.

After photobleaching, our model podosome recovers its fluorescence by incorporating actin-GFP monomers that come by diffusion from the cytoplasm outside of the bleached region. Experimentally, the cytosolic actin-GFP, considered monomeric, recovers by diffusion at least ten times faster than the fluorescence in the podosome, consistently with the diffusion coefficient for monomeric actin previously established (McGrath et al., 1998). Therefore, the fluorescence recovery of the podosome is not limited by the diffusion of the monomers. In the following, we will assume that diffusion is fast and we consider a bleached podosome surrounded by monomers that are all optically active. Due to the addition of fluorescent monomers, at time t after bleaching, a region of height h = r_0.v.t at the bottom of the podosome is fluorescent again. The total intensity of fluorescent light $I_t(t)$ measured at time t for one podosome is proportional to the of the podosome that has been re-polymerized:

$$I_t(t) \propto \sum_{i=0}^{n} I(i) \quad \text{with } n = vt \, .$$

The intensity $I_t(t)$ increases almost exponentially with time t (Fig. S4). The characteristic time τ relates to the synthesis and severing frequencies in a simple way :

$$\tau = \frac{1}{\sqrt{\beta v}} \qquad (4)$$

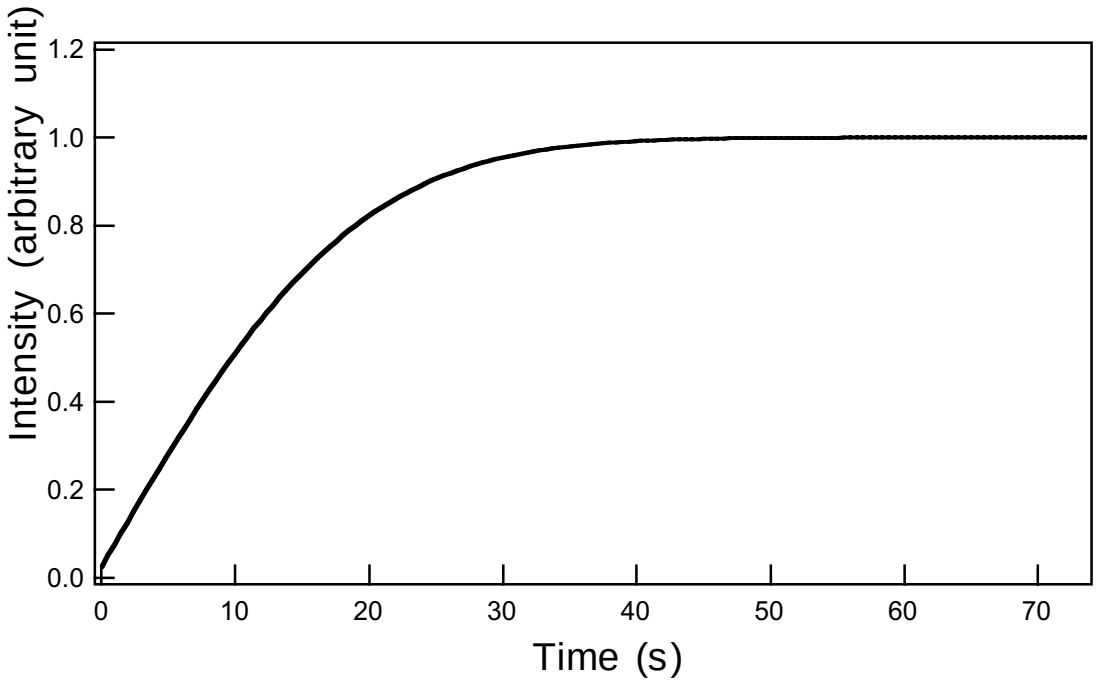

Figure S4 :Total intensity $I_t(t)$ of fluorescent light within a podosome as a function of time t after bleaching. Theoretical result with v= 3.1 Hz and $\beta = 3.6\ 10^{-4}$ Hz.

Experimental measurements of the synthesis velocity and severing frequency.

The podosomes have relatively constant characteristic dimensions with their height H, measured in the confocal microscope, of the order of 1 μm. A similar size of podosomes was measured by electron microscopy in v-src transformed fibroblasts (Gavazzi et al., 1989) and in osteoclasts (Ochoa et al., 2000). The FRAP characteristic time τ lies between 20 and 40 s. The ratio (H, Eq.3) and the product (τ, Eq.4) of v and β are therefore known and lead to $6 > v > 3$ Hz and $5.4\ 10^{-4}$ Hz $> \beta > 2.7\ 10^{-4}$ Hz. The growth frequency v corresponds then to synthesis velocities ranging from 0.5 μm/min to 1 μm/min.

Conclusions:

Our model uses two simple ingredients: the continuous polymerisation of actin filaments at the basis of the podosome and their equiprobable severing in the whole structure. Consistently, previous reports have shown the presence of actin polymerisation regulators at the basis of the podosome (Pfaff and Jurdic, 2001) and the presence of gelsolin, a protein with actin severing activity, in the podosome (Wang et al., 1984), (Chellaiah et al., 2000; Gavazzi et al., 1989). The model is consistent with an almost exponential shape for the FRAP curve for a single podosome and, interestingly, accounts for the steady typical height and apparent conical shape of the podosomes. Using the numerical values obtained experimentally, we also deduced from the model that the rate of polymerisation at the base of the podosome should be comprised between 0.5 and 1 $\mu m.min^{-1}$. Interestingly, these values are consistent with measurements of lamellipodial treadmilling in fibroblasts (0,79 +/- 0,31 $\mu m.min^{-1}$) (Wang, 1985) or of treadmilling in *Listeria* actin comets (Pantaloni et al., 2001) . An additional advantage of this model podosome is that it releases actin filaments that could readily account for the cloud of actin that surrounds it. Of course, this model probably oversimplifies many aspects of the podosome dynamics but it suggests that a relatively simple enzymatic equilibrium could regulate podosome structure.

Babb, S.G., P. Matsudaira, M. Sato, I. Correia, and S.S. Lim. 1997. Fimbrin in podosomes of monocyte-derived osteoclasts. *Cell Motil Cytoskeleton*. 37:308-25.

Chellaiah, M., N. Kizer, M. Silva, U. Alvarez, D. Kwiatkowski, and K.A. Hruska. 2000. Gelsolin deficiency blocks podosome assembly and produces increased bone mass and strength. *J Cell Biol*. 148:665-78.

Gavazzi, I., M.V. Nermut, and P.C. Marchisio. 1989. Ultrastructure and gold-immunolabelling of cell-substratum adhesions (podosomes) in RSV-transformed BHK cells. *J Cell Sci*. 94:85-99.

McGrath, J.L., J.H. Hartwig, Y. Tardy, and C.F. Dewey, Jr. 1998. Measuring actin dynamics in endothelial cells. *Microsc Res Tech*. 43:385-94.

Nermut, M.V., P. Eason, E.M. Hirst, and S. Kellie. 1991. Cell/substratum adhesions in RSV-transformed rat fibroblasts. *Exp Cell Res*. 193:382-97.

Nitsch, L., E. Gionti, R. Cancedda, and P.C. Marchisio. 1989. The podosomes of Rous sarcoma virus transformed chondrocytes show a peculiar ultrastructural organization. *Cell Biol Int Rep*. 13:919-26.

Ochoa, G.C., V.I. Slepnev, L. Neff, N. Ringstad, K. Takei, L. Daniell, W. Kim, H. Cao, M. McNiven, R. Baron, and P. De Camilli. 2000. A functional link between dynamin and the actin cytoskeleton at podosomes. *J Cell Biol*. 150:377-89.

Pantaloni, D., C. Le Clainche, and M.F. Carlier. 2001. Mechanism of actin-based motility. *Science*. 292:1502-6.

Pfaff, M., and P. Jurdic. 2001. Podosomes in osteoclast-like cells: structural analysis and cooperative roles of paxillin, proline-rich tyrosine kinase 2 (Pyk2) and integrin alphaVbeta3. *J Cell Sci*. 114:2775-86.

Wang, E., H.L. Yin, J.G. Krueger, L.A. Caliguiri, and I. Tamm. 1984. Unphosphorylated gelsolin is localized in regions of cell-substratum contact or attachment in Rous sarcoma virus-transformed rat cells. *J Cell Biol*. 98:761-71.

Wang, Y.L. 1985. Exchange of actin subunits at the leading edge of living fibroblasts: possible role of treadmilling. *J Cell Biol.* 101:597-602.